

Haemodynamic optimisation of a dialysis graft design using a global optimisation approach

Sjeng Quicken^{1,2}  | Tammo Delhaas¹  | Barend M. E. Mees³  |
Wouter Huberts^{1,2} 

¹Department of Biomedical Engineering, CARIM School for Cardiovascular Diseases, Maastricht University, Maastricht, The Netherlands

²Eindhoven University of Technology, Department of Biomedical Engineering, Eindhoven, Netherlands

³Department of Vascular Surgery, Maastricht University Medical Centre, Maastricht, the Netherlands

Correspondence

Wouter Huberts, Universiteitssingel 50, 6223ER Maastricht, The Netherlands.
Email: wouter.huberts@maastrichtuniversity.nl

Funding information

Chemelot InSciTe, Grant/Award Number: BM1.01; Dutch national e-infrastructure SURF Cooperative, Grant/Award Number: muc16272

Abstract

Disturbed flow and the resulting non-physiological wall shear stress (WSS) at the graft-vein anastomosis play an important role in arteriovenous graft (AVG) patency loss. Modifying graft geometry with helical features is a popular approach to minimise the occurrence of detrimental haemodynamics and to potentially increase graft longevity. Haemodynamic optimisation of AVGs typically requires many computationally expensive computational fluid dynamics (CFD) simulations to evaluate haemodynamic performance of different graft designs. In this study, we aimed to develop a haemodynamically optimised AVG by using an efficient meta-modelling approach. A training dataset containing CFD evaluations of 103 graft designs with helical features was used to develop computationally low-cost meta-models for haemodynamic metrics related to graft dysfunction. During optimisation, the meta-models replaced CFD simulations that were otherwise needed to evaluate the haemodynamic performance of possible graft designs. After optimisation, haemodynamic performance of the optimised graft design was verified using a CFD simulation. The obtained optimised graft design contained both a helical graft centreline and helical ridge. Using the optimised design, the magnitude of flow disturbances and the size of the anastomotic areas exposed to non-physiological WSS was successfully reduced compared to a regular straight graft. Our meta-modelling approach allowed to reduce the total number of CFD model evaluations required for our design optimisation by approximately a factor 2000. The applied efficient meta-modelling technique was successful in identifying an optimal, helical graft design at relatively low computational costs. Future studies should evaluate the in vivo benefits of the developed graft design.

Abbreviations: agPCE, adaptive generalised polynomial chaos expansion; AVG, arteriovenous graft; CFD, computational fluid dynamics; CTA, computed tomography angiography; NIH, neointimal hyperplasia; OSI, oscillatory shear index; TAWSS, time averaged wall shear stress; WSS, wall shear stress.

This is an open access article under the terms of the Creative Commons Attribution-NonCommercial License, which permits use, distribution and reproduction in any medium, provided the original work is properly cited and is not used for commercial purposes.

© 2020 The Authors. *International Journal for Numerical Methods in Biomedical Engineering* published by John Wiley & Sons Ltd.

KEYWORDS

arteriovenous grafts, computational fluid dynamics, geometric optimisation, polynomial chaos expansion, sensitivity analysis

1 | INTRODUCTION

The main cause for dysfunction of arteriovenous grafts (AVG) for haemodialysis is neointimal hyperplasia (NIH) at the graft-vein anastomosis, causing stenosis and low flow, ultimately resulting in thrombosis and graft patency loss. NIH development is believed to be triggered by disturbed blood flow and non-physiological wall shear stresses (WSS) around the venous anastomosis.^{1,2} Although the exact haemodynamic trigger for NIH development is unknown,³ various novel graft designs have been proposed to reduce disturbed flow and non-physiological WSS at the graft-vein anastomosis.⁴

One promising approach to optimise haemodynamics aims at inducing helical blood flow patterns near the venous anastomosis. Helical flow is a physiologically occurring phenomenon⁵ and is hypothesised to stabilise flow and to result in favourable WSS conditions.^{6,7} Graft designs that induce helical flow either exhibit a helical graft centreline,⁸ or a helical ridge that extrudes into the graft's lumen.⁹ Early clinical studies indeed suggest that both helical graft designs improve in vivo graft performance.^{9,10}

Previous computational fluid dynamics (CFD) simulation studies also demonstrated that helical graft designs can improve haemodynamic conditions near the graft-vein anastomosis.¹¹⁻¹³ However, finding the optimal helical graft design is complicated because anastomotic haemodynamics not only directly depend on the design parameters (e.g., helical pitch, ridge height, graft diameter), but also on interactions between design parameters.¹¹⁻¹³ Hence, graft design parameters cannot be optimised one factor at a time, as the haemodynamic effect of one parameter could be highly dependent on the specific value of any of the other parameters. A global optimisation approach is therefore required, in which all parameters are optimised simultaneously. However, such a global optimisation requires evaluation of the haemodynamic performance of a large range of different graft designs, which is hampered by the high computational costs of individual CFD simulations.

A meta-modelling technique could be useful to allow for efficient, global graft optimisation.¹⁴ A meta-model (i.e., a model of a model) is typically constructed from a limited training dataset containing computationally expensive CFD simulations and should subsequently be able to predict haemodynamic graft performance for design parameter combinations that are not included in the training dataset. Because a meta-model can be evaluated at a low computational cost, it can serve as an efficient substitute for the CFD model during global optimisation.

In the field of engineering, several types of meta-modelling techniques are available, such as polynomial models or Gaussian Kriging models.¹⁴ In this study, we propose a meta-modelling approach based on the adaptive generalised polynomial chaos expansion (agPCE),¹⁵ recently developed for the purpose of efficient uncertainty quantification and sensitivity analysis for computationally expensive biomedical models.¹⁶ Though agPCE meta-models are typically used to assess how model input uncertainty translates to a stochastic model output, we hypothesise it can also be used to predict how different helical graft design parameter settings translate to haemodynamic graft performance. In addition, the use of agPCE meta-models allows for the analytical assessment of the magnitude of design parameter interactions and the relative importance of each parameter with respect to the model output.¹⁷ Such an analysis is useful for design optimisation, because it can be used to assess which parameters are most rewarding to optimise.

The aim of this study was to develop a haemodynamically optimised AVG design using the efficient agPCE meta-modelling approach. During optimisation, a helical graft centreline and/or helical ridge could be added to the graft design when its inclusion would benefit haemodynamic graft performance. The haemodynamic performance of the optimised graft design was finally verified by a CFD simulation.

2 | MATERIALS AND METHODS

2.1 | Brief summary of graft design optimisation strategy

A realistic reference AVG geometry was created from 15 months post-operative computed tomography angiography (CTA) imaging. These scans were obtained for diagnostic purposes during graft follow-up. Clinical evaluation of the CTA revealed

a non-significant stenosis in the venous anastomotic region. It was assumed that this stenosis did not impact vessel path or anastomotic configuration. All measurements were performed at the Maastricht University Medical Centre (Maastricht, the Netherlands). A waiver for ethical approval of this study was obtained from the local medical ethical committee.

Apart from vessel path (i.e., vessel path and anastomotic configuration), the reference geometry was fully parametrised, which facilitated implementation of grafts with a possible helical centreline and/or a helical ridge. Several design parameters were established to define graft design.

Next, a dataset was created that contained CFD evaluations of various uniquely sampled 3D graft designs. Using the information from this dataset, meta-models were created to relate graft design parameters to anastomotic haemodynamics. These meta-models were first used to identify those design parameters that were relevant for graft performance and that thus should be considered during optimisation. Next, using the meta-models to predict venous anastomotic haemodynamics, an optimal graft design was proposed. The optimised graft design's haemodynamic performance was finally verified using a full-scale CFD simulation.

2.2 | A realistic parametrised AVG geometry

2.2.1 | Reference AVG geometry

The graft and adjacent artery and vein were segmented from the CTA dataset using the software package VMTK.¹⁸ Subsequently, the vessels' centrelines were extracted to define global vessel path and were exported to SolidWorks 2018 (Dassault Systèmes, Vélizy-Villacoublay, France). Here, vessels with constant diameter were imposed on the centrelines. To approximate the graft geometry prior to vessel remodelling, venous and arterial diameter were estimated from 2 weeks-preoperative ultrasound examination and set to 7.7 and 6.6 mm, respectively. Proximal to the anastomosis, the arterial and venous segments were cut to 7.5 times the respective diameter, whereas vessel segments distal to the anastomosis were cut to 1.0 times the respective diameter. Straight flow extensions were subsequently added to all arterial and venous vessel segments, to reduce the influence of boundary condition assumptions on the simulation output.¹⁹ Using these flow extensions, the vessel segments proximal to the anastomosis had a length of 15 times the respective diameter, whereas distal to the anastomosis vessel segments had a length of 6.5 times the respective diameter.

2.2.2 | Creation of a helical graft design

The baseline AVG geometry was extended to incorporate a helical graft centreline and/or a helical ridge in the graft's lumen. The helical graft centreline was defined by specification of a helical pitch (p) and amplitude (A) (Figure 1A,B, respectively). The helical ridge shared the same pitch as that of the helical graft centreline and was implemented as two opposing elliptical cuts in the graft's cross-section (Figure 1B). The depth and width of the helical ridge were defined by the ellipse's major (h) and minor axis, respectively. Since the ellipse's major axis was hypothesised to be of more importance to anastomotic haemodynamics than its minor axis,¹² the ratio between the major and minor axis of the elliptical cut was set as 3:2. Note that when A and h were zero, a straight graft was created.

To compensate for possibly increased flow resistance due to the helical features,^{11,20} graft diameter (D) could be increased with respect to the standard diameter used for dialysis grafts (i.e., 6.0 mm). Finally, the helical graft could be rotated along its axial axis with angle α , which changed the location of the trailing edges of the helical ridge at both the arterial and venous anastomosis and the exact anastomotic angle (Figure 1A). At an angle α equal to 0° or 180° , the trailing edges of the helical ridge were perpendicular to the venous centreline (i.e., on the side of the vein), whereas at an angle of 90° or 270° they were parallel to the venous centreline (i.e., on the distal and proximal side of the anastomosis).

2.3 | Meta-model development

2.3.1 | Design of experiments

Relevant ranges were defined for all graft design parameters (Table 1), which were either assumed or based on available literature. Subsequently, a meta-model training dataset was created by generating unique, uniformly distributed input

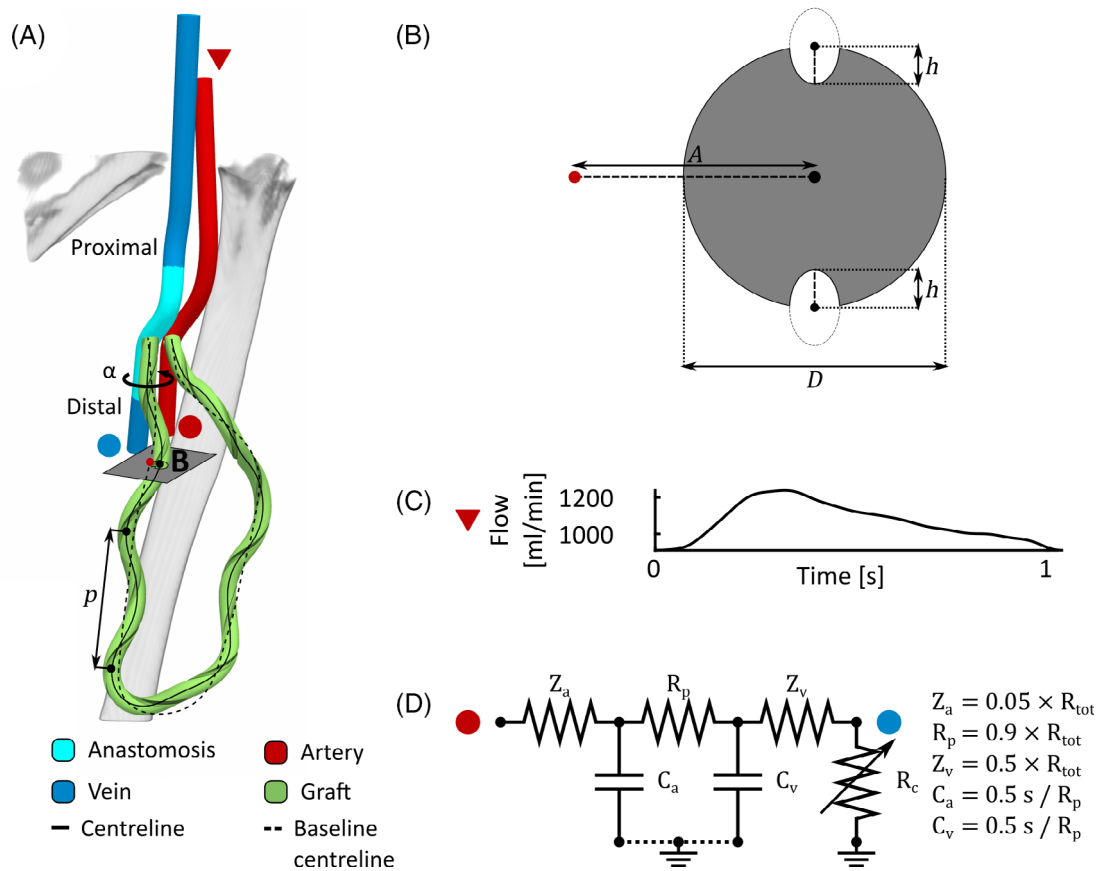


FIGURE 1 Overview of the helical graft and model parameters (A and B), the arterial inflow boundary condition (C) and the peripheral vasculature boundary condition model (D). (D) Z_a and Z_v represent the arterial and venous characteristic impedances to couple the boundary condition model to the 3D domain. The peripheral resistance is indicated by R_p , whereas C_a and C_v indicate the compliance of the arterial and venous systems, respectively. The flow over the collateral veins is regulated by the adjustable resistor R_c

Parameter	Reference graft	Min	Max	Range based on
Graft diameter (D)	6.0 mm	6.0 mm	6.5 mm	Assumed
Helical pitch (p)	N/A	4.0 mm	10.0 mm	11
Helical amplitude (A)	0.0	0.0	$0.75 \cdot D$	Assumed
Ridge height (h)	0.0	0.0	$0.3 \cdot D$	12
Graft orientation (α)	N/A	0°	360°	12

TABLE 1 Graft design parameter ranges

Note: The helical amplitude (A) and ridge height (h) are a function of graft diameter (D).

samples within the graft design input domain using Sobol's low discrepancy series.²¹ For each input sample, the corresponding graft geometry was generated automatically. Note that due to Sobol sampling, the training dataset also contained a sample at the lower limit of all parameters. Hence, a sample was generated with a diameter of 6 mm and a helical amplitude and ridge height which were both equal to zero. This sample corresponded to a standard, 6 mm, non-helical graft design. The haemodynamic performance of this graft design was used as a reference for graft performance throughout this study (Table 1).

The helical ridge height was set to zero in any geometry in the training dataset where h was smaller than 3.75% of the graft's diameter. In these cases, the ridge was removed because it was hypothesised that its inclusion would insignificantly contribute to overall haemodynamics, whereas it would significantly increase the number of mesh elements that were required to accurately track the graft's surface.

2.3.2 | CFD simulations

Blood flow simulations were performed for all AVG geometries in the training dataset using the open source Navier–Stokes solver OASIS,²² implemented in the finite element package FEniCS.²³ Blood was regarded as a Newtonian fluid with a dynamic viscosity of 3.5×10^{-3} Pa·s and a density of 1050 kg/m^3 . Flow was considered laminar, as preliminary testing showed that adding a turbulence model had negligible impact on the haemodynamic metrics of interest (non-published results). Computational meshes of the AVG geometries were created using Fluent 19.1 (Ansys, Canonsburg, PA, USA). Mesh density was increased near the anastomoses to locally increase solver accuracy. Global meshing settings were obtained from a mesh convergence study on the reference AVG geometry and resulted in meshes containing 2.7×10^6 – 4.7×10^6 second order tetrahedral Taylor-Hood elements. Simulations were progressed in time using step sizes of 10^{-4} s. The time step was reduced to $\frac{2}{3} \times 10^{-4}$ s whenever the simulation failed to converge.

Boundary conditions: Flow at the arterial inlet was prescribed using a time-dependent blunt velocity profile, as described in Smith et al.²⁴ An arteriovenous coupling model was prescribed at the distal arterial and venous boundaries to mimic the peripheral vasculature (Figure 1D). This coupling model contained a variable resistor R_c that bypassed the venous segment of the CFD model, to represent any collateral vein that might be present in the patient. It was assumed that flow was divided equally between the 3D modelled vein and the collaterals. Venous outlet pressure was assumed constant and was set to 0 mmHg.

It was assumed that, in order to maintain sufficient tissue perfusion, time averaged flow toward the peripheral vasculature distal to the anastomosis would not be influenced by AVG creation. Hence, flow magnitude prescribed at the arterial inlet was computed as the sum of the 7 week-postoperative (pulsatile) graft flow and the 2 week-preoperative (average) brachial artery flow, as measured by duplex ultrasound, resulting in an average flow of $1.06 \times 10^3 \text{ mL/min}$ (Figure 1C). The sum of all resistive elements of the arteriovenous coupling model (R_{tot}) was fitted to ensure that time averaged flow through the arteriovenous coupling model equalled the preoperative brachial artery flow (73 mL/min).

2.3.3 | Graft haemodynamic performance metrics

Haemodynamic metrics were defined to quantify disturbed flow and non-physiological WSS in the anastomotic region. Although multiple hypotheses regarding the definition of disturbed WSS exist,³ here it was assumed that WSS outside the physiological range (<0.1 or $>7 \text{ Pa}^{25}$), WSS sufficiently high to cause irreversible endothelial damage ($>40 \text{ Pa}^{26}$) and highly oscillatory WSS were detrimental to graft longevity. All WSS metrics were computed only in the venous anastomosis, which was defined as the region ranging from 2.5 cm distal to the anastomosis to 3.0 cm proximal of the anastomosis (Figure 1A). Furthermore, since arterial inflow was equal for all simulations, the average pressure drop from the model's arterial inlet to the venous outlet (Δp) was computed as a measure of the graft's flow resistance. All metrics were computed over the third simulated cardiac cycle.

Exposure to non-physiologically low WSS ($<0.1 \text{ Pa}$) was assessed by computing the time averaged WSS (TAWSS):

$$\text{TAWSS} = \frac{1}{T} \int_{t=0}^{t=T} \left\| \vec{\tau}(t, \vec{x}) \right\| dt \quad (1)$$

where $\vec{\tau}(t, \vec{x})$ represents the local WSS vector and T is the duration of the cardiac cycle. Exposure to non-physiologically low WSS was quantified by computing the percentage of the anastomotic area where $\text{TAWSS} < 0.1 \text{ Pa}$ ($\% \text{WSS}_{<0.1 \text{ Pa}}$).

Exposure to non-physiologically high WSS ($>7 - \leq 40 \text{ Pa}$) and WSS sufficiently high to cause irreversible endothelial damage ($>40 \text{ Pa}$) were assessed by computing WSS_{max} :

$$\text{WSS}_{\text{max}} = \max \left\{ \left\| \vec{\tau}(t, \vec{x}) \right\| : t = 0 \dots T \right\} \quad (2)$$

Exposure to high and very high WSS were quantified by computing the percentage of the anastomotic surface area exposed to WSS_{max} in excess of 7 Pa ($\% \text{WSS}_{>7 \text{ Pa}}$) and the percentage of the anastomotic surface area exposed to WSS_{max} in excess of 40 Pa ($\% \text{WSS}_{>40 \text{ Pa}}$).

Oscillatory WSS was evaluated by computing the oscillatory shear index²⁷ (OSI):

$$\text{OSI} = \frac{1}{2} \left(1 - \frac{\left\| \int_{t=0}^{t=T} \vec{\tau}(t, \vec{x}) dt \right\|}{\int_{t=0}^{t=T} \left\| \vec{\tau}(t, \vec{x}) \right\| dt} \right) \quad (3)$$

that ranges between 0 and 0.5. Exposure to highly oscillatory WSS was quantified by computing the percentage of the anastomotic region where $\text{OSI} > 0.25$ ($\% \text{OSI}_{>0.25}$).

Disturbed flow and/or turbulence in the venous segment was evaluated by computing the root-mean-square magnitude of high frequency velocity perturbations. Hereto, Reynolds decomposition was applied to decompose the local flow velocity magnitude $\vec{u}(t, \vec{x})$ into an average trend and into high frequency velocity perturbations ($\tilde{u}(t, \vec{x})$). Subsequently, $\tilde{u}_{\text{RMS}}(t, \vec{x})$ was computed as the root-mean-square value of $\tilde{u}(t, \vec{x})$ over the cardiac cycle. The changes in $\tilde{u}_{\text{RMS}}(t, \vec{x})$ along the venous segment was assessed by computing its cross-sectional median value perpendicular to the centreline: $\tilde{u}_{\text{RMS},50}(t, \vec{x})$. Finally, the maximum value of $\tilde{u}_{\text{RMS},50}(t, \vec{x})$ along the venous segment ($\tilde{u}_{\text{max}}(t, \vec{x})$) was used as a proxy for the amount of disturbed flow in each simulation.

2.3.4 | Meta-model creation

For each of the graft geometries in the training dataset, haemodynamics were evaluated using the six metrics defined in the previous subsection. Subsequently, based on the evaluations of all simulations in the training dataset, individual meta-models were created for the total output domain Y_i of each of the six haemodynamic metrics, by means of an adaptive generalised polynomial chaos expansion (agPCE) method.²⁸ This method expanded the output domain of each haemodynamic metric (Y_i) into a set of multivariate orthogonal polynomials that were a function of the graft design parameters:

$$Y_i = f_i(\mathbf{X}) \approx f_{i,\text{PCE}}(\mathbf{X}) = \sum_{j=1}^{N_p} c_j \psi_j(\mathbf{X}). \quad (4)$$

Here, $\psi_j(\mathbf{X})$ and c_j represent the polynomials and their expansion coefficients, respectively. Furthermore, \mathbf{X} represents the set of CFD model input parameters (D , A , p , h , and α) that were defined on the model input domain.

Legendre polynomials were chosen as the basis polynomials of the meta-model, since they are best suited for models with uniformly sampled input.²⁹ The meta-model's expansion coefficients were estimated using least-square-regression. To prevent possible overfitting of the data by the meta-model, the maximum number of meta-model polynomials was limited to half the number of CFD model evaluations in the training dataset.¹⁶

An adaptive algorithm^{15,16} was used to only include those polynomials into the meta-model that significantly increased its quality. As such, this method allowed for creation of high-quality meta-models, while keeping the required training dataset as small as possible. An extensive overview of this algorithm is presented in Quicken et al.¹⁶ The quality of the final meta-model was assessed by computing the leave-one-out cross validation coefficient Q^2 , that ranges between 0 and 1, for low and high-quality meta-models, respectively.

2.4 | Geometry optimisation

2.4.1 | Identification of important design parameters

Design parameters relevant for graft optimisation were first identified using sensitivity analysis. For this purpose, the main and total Sobol sensitivity indices (S and S_T , respectively) of each design parameter were computed for all six haemodynamic metrics for graft performance. Both sensitivity indices could be derived analytically from the agPCE meta-models.¹⁷ The main Sobol sensitivity index is a measure for variance in a haemodynamic output that can be attributed directly to a single design parameter, whereas the total sensitivity index also includes the contributions of

interactions between parameters. As such, for each design parameter, the difference $S_T - S$ is a measure for interactions this parameter has with other design parameters. Both S and S_T range between 0 and 1.

Whenever the total sensitivity index of a design parameter was below 0.05 for all haemodynamic metrics, the parameter was deemed insignificant to the graft's haemodynamic performance and subsequently omitted during graft optimisation.

2.4.2 | Objective function

Objective functions were defined for each of the six haemodynamic metrics for graft performance. These objective functions were defined such that they reduced to zero when a predefined target value had been reached. Furthermore, the objective function of the pressure drop exceeded 1 when pressure drop deviated more than 1 mmHg from the target value. For all other parameters, the objective function exceeded one when graft performance was worse than the reference graft design (i.e., a 6 mm straight graft).

It was assumed that the flow resistance of the optimised graft should be equal to that of the reference graft, since this would minimise the chance for a too high or too low blood flow through the graft. Therefore, the target value for the pressure drop (Δp_{target}) was set equal to the pressure drop over the reference straight dialysis graft design. Because the meta-models' predictive power outside the training dataset's output domains were unknown, the target value for all other parameters ($Y_{i,\text{target}}$) was chosen as the minimum observed value in any of the training CFD simulations. Consequently, the objective function for Δp was defined as:

$$O_{\Delta p} = \left(\frac{\Delta p - \Delta p_{\text{target}}}{\Delta p_0} \right)^2 \quad (5)$$

in which Δp_0 is thus set to 1 mmHg. For all other parameters the objective function is assumed to have the form:

$$O_{Y_i} = \left(\frac{Y_i - Y_{i,\text{target}}}{Y_{i,\text{ref}} - Y_{i,\text{target}}} \right)^2 \quad (6)$$

Finally, a joined objective function was defined to evaluate the grafts overall haemodynamic performance:

$$O_{\text{tot}} = \sum_{i=1}^6 w_i O_{Y_i} \quad (7)$$

where w_i represents a weighting of each individual objective function. Since it is unknown which of the computed haemodynamics metrics is the most important factor in graft dysfunction,³ all objective functions were weighted equally by setting $w_i = 1$. Consequently, O_{tot} equated to 5 for the reference graft design. Any value larger than 5 indicated an overall deterioration of haemodynamic graft performance with respect to the reference graft, whereas a value lower than 5 indicated improved haemodynamic performance. Hence, minimising the objective function aims to reduce high frequency velocity perturbation as well as the percentage of the anastomotic area exposed to low time averaged WSS (< 0.1 Pa), to non-physiologically high maximum WSS ($>7 - \leq 40$ Pa), to maximum WSS sufficiently high to cause irreversible endothelial damage ($\text{WSS}_{\text{max}} > 40$ Pa) and to highly oscillatory WSS ($\text{OSI} > 0.5$), while simultaneously ensuring that the pressure drop over the graft is similar to that over a standard straight graft.

2.4.3 | Optimisation algorithm

Graft optimisation was performed by applying the sequential quadratic programming method, as implemented in the optimisation toolbox of MATLAB 2018a (the MathWorks, Natick, MA, USA), to minimise (7). Parameter values during optimisation were constraint to the ranges defined in Table 1. During optimisation, the objective function was evaluated

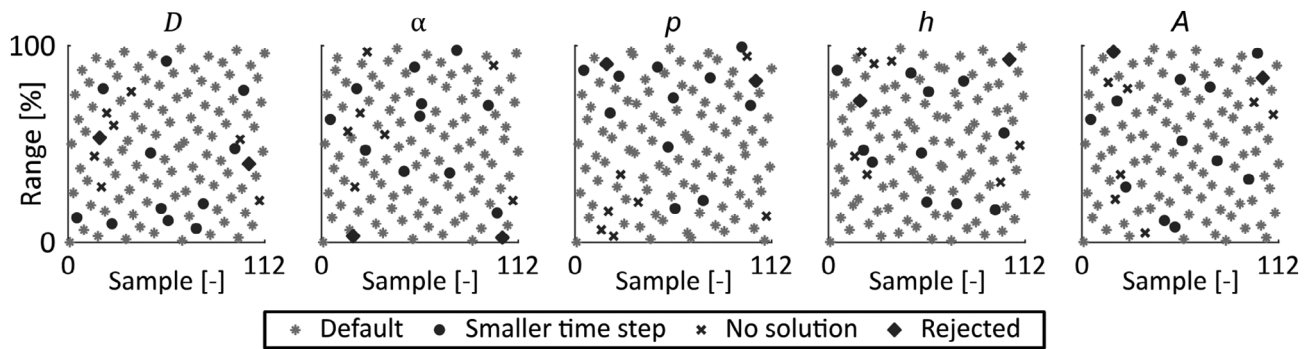


FIGURE 2 Overview of the generated samples for all model input parameters and the simulation result per sample

using meta-model predictions for each of the six haemodynamic metrics for graft performance. To prevent that local minima were found for (7), the optimisation was initiated from 1000 randomly chosen starting points. Note that the optimisation algorithm could still exclude the helical ridge or helical centreline when its inclusion would not benefit haemodynamic graft performance, by setting either h or D to zero.

After optimisation, the haemodynamic performance of the optimised graft design was verified by performing a full-scale CFD simulation as described in Section 2.3.2.

Apart from vessel path (i.e., vessel path and anastomotic configuration), the reference geometry was fully parametrised, which facilitated implementation of grafts with a possible helical centreline and/or a helical ridge. Several design parameters were established to define graft design.

3 | RESULTS

3.1 | CFD simulations

A total of 112 AVG geometries were generated using the experimental design from Section 3.3. Two of these geometries were rejected due to overlap of the arterial and venous graft segments. Of the remaining 110 geometries, 92 simulations were run using time-stepping size of 10^{-4} s, 11 simulations were run using a time-stepping size of $\frac{2}{3} \times 10^{-4}$ s (Figure 2). For one simulation, the Navier–Stokes solver failed to converge after simulating 2.4 s. Six simulations crashed already within a simulation time of 10^{-2} s, probably related to problems with the mesh. The samples of the failed simulations were scattered over the total input domains of D , A , p , h , and α , but it was observed that the pitch p of these simulation tended toward its lower limit (Figure 2). Consequently, the complete input domain of all parameters was covered. The simulations that showed overlap between the arterial and venous graft segments and the simulations that crashed were omitted from further processing. As such, a total of 103 successful simulations were performed. Average simulation time of each CFD simulation was 77 hours on machines with either 24 or 32 processor cores.

3.2 | Haemodynamic metrics

In the reference simulation, the pressure drop over the geometry, Δp , was equal to 1.96×10^3 Pa (14.7 mmHg). The values of $\%WSS_{<0.1\text{Pa}}$, $\%WSS_{>7\text{Pa}}$, $\%WSS_{>40\text{Pa}}$ and $OSI_{>0.25}$ were 30.2%, 55.0%, 1.2%, 4.0%, respectively. The maximum velocity perturbation metric $\tilde{u}_{\max}(t, \vec{x})$ of the reference simulation equalled 6.0 cm/s (Figure 3).

In the simulations in the training dataset, the pressure drop over the geometry ranged from 1.6×10^3 Pa to 3.4×10^3 Pa (12–26 mmHg). The value of $\tilde{u}_{\max}(t, \vec{x})$ was between 4.1–8.7 cm/s. The percentage of the anastomotic area exposed to low WSS (<0.1 Pa) ranged between 4.1%–33.4%, whereas the percentage of the anastomotic areas exposed to high WSS (>7 – ≤ 40 Pa) and very high WSS (>40 Pa) ranged between 49.9%–61.6% and 0.0%–3.8%, respectively. Furthermore, the area exposed to highly oscillating WSS ($OSI > 0.25$) in the helical AVG simulations was between 1.1%–8.7%.

Haemodynamic performance of the graft designs in the training dataset, as expressed by the objective function in (7), ranged between 2.4–130.8.

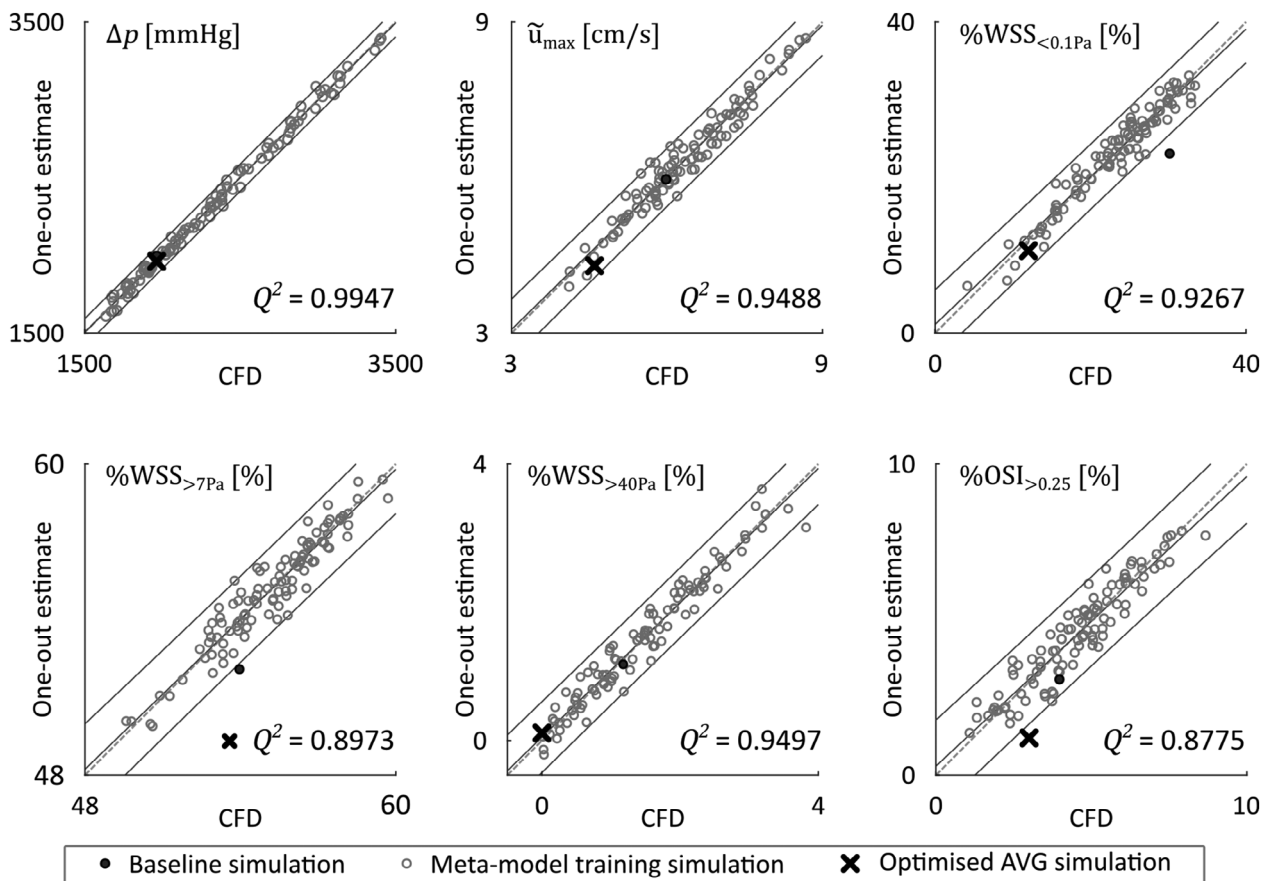


FIGURE 3 Overview of the meta-models' Q^2 values and the meta-model prediction (leave-one-out estimate), versus the CFD output for the training dataset (including the reference simulation) and the final optimised AVG geometry. The solid diagonal lines indicate the 95% confidence interval of the data, whereas the diagonal striped lines indicate the line of identity

TABLE 2 Overview of the total sensitivity indices and the contribution of parameter interactions ($S_T - S$) for each haemodynamic metric for graft performance

Parameter	S_T					$S_T - S$				
	D	α	p	h	A	D	α	p	h	A
Δp	0.10	0.02	0.06	0.85	0.05	0.02	0.02	0.04	0.03	0.03
$\tilde{u}_{\max}(t, \vec{x})$	0.32	0.43	0.29	0.37	0.42	0.22	0.27	0.26	0.30	0.39
%WSS _{<0.1Pa}	0.20	0.43	0.38	0.36	0.42	0.18	0.21	0.37	0.32	0.35
%WSS _{>7Pa}	0.35	0.63	0.33	0.42	0.43	0.32	0.56	0.26	0.38	0.42
%WSS _{>40Pa}	0.37	0.39	0.30	0.39	0.24	0.25	0.20	0.27	0.26	0.24
OSI _{>0.25}	0.20	0.30	0.45	0.61	0.54	0.17	0.27	0.39	0.60	0.54

Note: For each haemodynamic output metric, the parameter with the highest total sensitivity index is indicated in boldface.

3.3 | Meta-modelling

Meta-models of the six haemodynamic metrics for graft performance were successfully created. The meta-model of Δp was obtained with a Q^2 larger than 0.99. The final meta-models of $\tilde{u}_{\max}(t, \vec{x})$, %WSS_{<0.1Pa} and %WSS_{>40Pa} had values of Q^2 between 0.9 and 0.95. The meta-models for OSI_{>0.25} and %WSS_{>7Pa} had values of Q^2 between 0.87 and 0.90 (Figure 3).

All input parameters showed total sensitivity indices that were above 0.05 for at least five of the haemodynamic output metrics (Table 2). Consequently, all input parameters were deemed relevant for graft performance and considered

during global graft design optimisation. Furthermore, large interactions ($[S_T - S] > 0.05$) between design parameters were observed for all output metrics except Δp (Table 2), which emphasises the need for our global optimisation strategy.

3.4 | Optimisation

An optimised graft geometry design was identified using the methods described in Section 2.4. This design had a graft diameter D of 6.4 mm, a helical pitch p of 4.7 cm and a ridge height h of 2.4×10^{-1} mm (i.e., 3.75% of D). Furthermore, helical amplitude A was equal to 0.36 cm and graft rotation angle α was set to 93° (Figure 4). The optimisation procedure finished within 4.5 minutes and required a total number of 2.1×10^5 meta-model evaluations to be performed.

In the CFD simulation of the optimised graft, all haemodynamic metrics showed improvements compared to the reference AVG design (Figure 4 and Table 3). More specifically, the maximum observed value for $\tilde{u}_{\max}(t, \vec{x})$ was reduced by approximately 25% with respect to the reference graft, whereas the area exposed to low WSS was reduced by a factor 3. Furthermore, the area exposed to highly oscillating WSS was reduced by 25%, whereas WSS in excess of

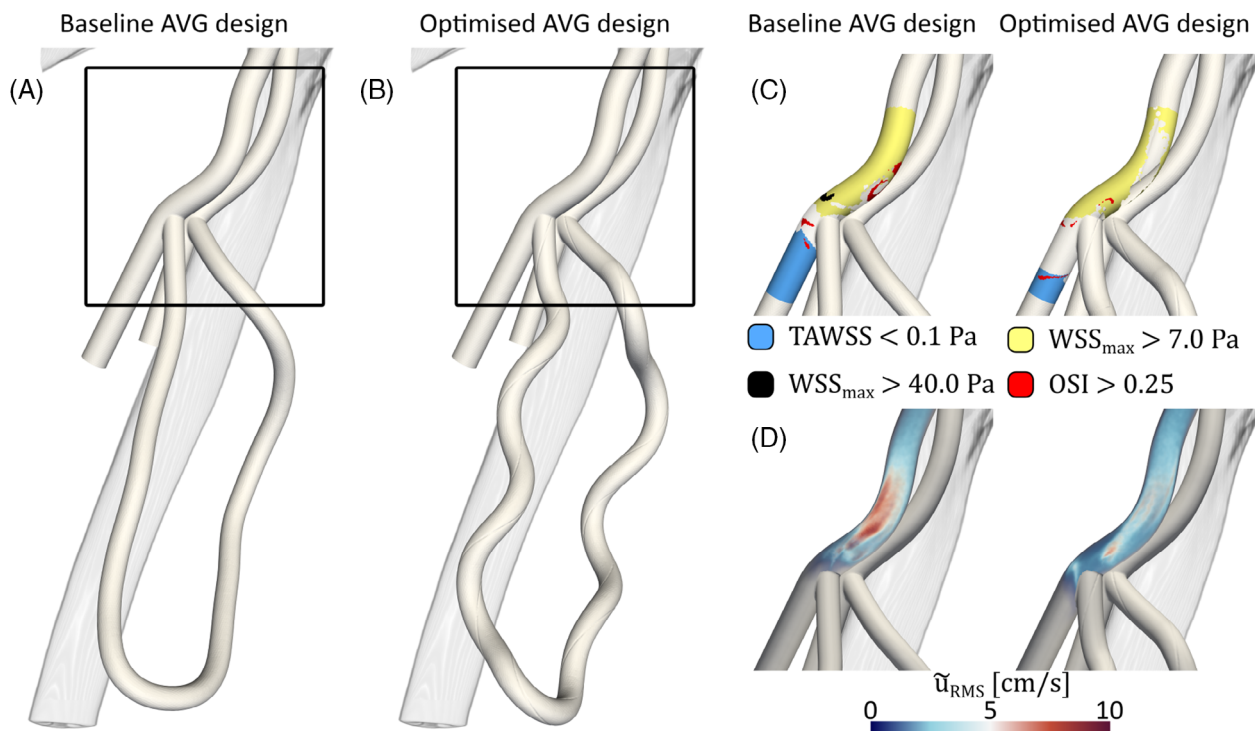


FIGURE 4 Comparison between the reference and the optimised graft design (A and B), Comparison between the WSS metrics (C) and the flow perturbations (D) in the two graft designs

Parameter	Meta-model	CFD	Reference
O_{tot}	0.084	1.41	5
Δp	1.96×10^3 Pa	1.96×10^3 Pa	1.96×10^3 Pa
$\tilde{u}_{\max}(t, \vec{x})$	$4.3 \text{ cm} \cdot \text{s}^{-1}$	$4.6 \text{ cm} \cdot \text{s}^{-1}$	$6.0 \text{ cm} \cdot \text{s}^{-1}$
%WSS $_{<0.1\text{Pa}}$	10.6%	12.0%	30.2%
%WSS $_{>7\text{Pa}}$	49.5%	54.5%	55.0%
%WSS $_{>40\text{Pa}}$	0.1%	0%	1.2%
OSI $_{>0.25}$	1.2%	3.0%	4.0%

TABLE 3 Meta-model predicted graft performance versus graft performance in CFD and the reference graft design

40 Pa was completely absent. Only a slight reduction (0.5%) in the anastomotic area exposed to WSS above 7 Pa with respect to the reference graft was observed (Table 3).

The values of Δp , $\tilde{u}_{\max}(t, \bar{x})$, %WSS_{<0.1Pa} and %WSS_{>40Pa} of the CFD model evaluation of the optimised graft were within the 95% confidence interval of the meta-model error (Figure 3). Larger discrepancies between the CFD model and the meta-model prediction were observed for %WSS_{>7Pa} and OSI_{>0.25}. The objective function of the optimised graft's was higher when evaluated by CFD than what was predicted by the meta-model (Table 3). However, the objective function value was still lower than that of the best performing AVG geometry in the meta-model training set.

4 | DISCUSSION

The aim of this study was to develop a haemodynamically optimised graft design using an efficient agPCE meta-modelling method. This approach allowed to analytically perform global parameter sensitivity analysis, which was used to identify which graft design parameters could be omitted from the graft optimisation procedure. Using this approach, a haemodynamically optimised graft design was developed that contained helical features. Since these features were not enforced during optimisation, the fact that the optimisation algorithm did include them in the final design supports earlier observations^{9,10} that helical graft features can be used to optimise AVG haemodynamics.

Global sensitivity analysis revealed that all graft design parameters had a significant effect on at least five of the metrics for haemodynamic graft performance. Furthermore, large interactions between design parameters were observed for all haemodynamic output metrics except Δp . Because of the observed interactions, the effect of each parameter on the haemodynamic performance of a graft is highly dependent on the settings of the other design parameters. This could be a possible explanation for the fact that earlier studies in helical graft designs concluded that no clear relations between design parameters and the observed haemodynamic effect could be identified.¹¹ Furthermore, due to the high sensitivity of blood flow to local geometric characteristics, it is expected that large parameter interactions will generally be present in graft designs. As such it is likely impossible to optimise graft design one parameter at a time. Instead, all graft design parameters need to be optimised simultaneously, which advocates for an approach as presented in this study.

In this study it was found that the haemodynamic metrics for graft performance were most impacted by the choice for the graft's rotation α and/or the helical ridge height h . The relative importance of graft rotation angle α is in agreement with other CFD studies on helical grafts.^{12,30} However, the choice for the graft's rotation angle is arguably the hardest to implement in the design of the graft and, without any precautions to ensure its value, is probably dictated by the surgical procedure and the anatomical patient characteristics. Consequently, it is likely beneficial for future research to focus on either devising a method to fix α into the graft design, or to minimise its impact on graft performance. Furthermore, the importance of h suggests that the helical ridge is more important in graft performance than a helical graft centreline. This contrasts to findings of earlier studies,^{13,30} that concluded that the haemodynamic effect of a helical graft centreline is much larger than that of the helical ridge. Though this may be explained by the fact that a different (patient-based) graft model was used in this study instead of a generic model, another possible explanation for this discrepancy could be that only local sensitivity analysis was performed in the aforementioned studies^{13,30} (i.e., all design parameters were modified one by one). This underlines the importance of applying global sensitivity analysis techniques when a model potentially contains many parameter interactions.

Opposed to most studies on the effect of graft design on anastomotic haemodynamics in idealised geometries,^{11,12} a patient-specific AVG geometry was used in this study. Since haemodynamics are highly dependent on local geometrical variations, we believe this patient-specific approach is more representative of the in vivo situation. However, as graft performance might also be dependent on patient-specific vessel characteristics, future studies should evaluate whether the haemodynamic performance benefit of the proposed graft design is maintained in other patient-specific vessel geometries, or whether a more generally applicable graft design should be developed.

During graft design optimisation an efficient agPCE meta-model was used instead of CFD simulations to predict how haemodynamic metrics related to graft dysfunction were impacted by graft design characteristics. To build the meta-model, a training dataset containing a total of 103 CFD model evaluations was used. Since each CFD model took on average 77 hrs to complete, creating the training dataset for the meta-model creation required a considerable amount of computational resources. However, since the graft optimisation algorithm used in this study required more than 200,000 model evaluations, the meta-modelling approach used in this study allowed to reduce the total number of

CFD model evaluations required for design optimisation by approximately a factor 2000. While the total number of model evaluations required during the optimisation procedure may be reduced considerably by employing a different optimisation algorithm, it is expected that the computational benefits of using a meta-model during optimisation will persistently outweigh the computational costs of meta-model creation. While the proposed optimisation approach was applied in the context of graft design optimisation, it is hypothesised that it will also be beneficial to a large range of other optimisation problems that would traditionally require a large number of computationally expensive model evaluations to be performed.

While the agPCE-based meta-modelling approach used in this study could be used to efficiently propose a haemodynamically optimised graft design, other meta-modelling approaches have also been suggested. For instance, in a study by Grechy et al.³¹ a Kriging-based meta-modelling approach was used to successfully optimise haemodynamics in an arteriovenous fistula model using a similar number of computationally expensive CFD simulations as were used in this study. However, it is unclear if the method used by Grechy et al. also allows for a global sensitivity analysis prior to optimisation. A global sensitivity analysis considers model parameter interactions and is useful for simplifying the final optimised design by removing irrelevant features from the optimisation procedure. Nonetheless, it should be evaluated in future research how the performance of the method proposed by Grechy et al. and the one proposed in this study compare.

4.1 | Limitations

In this study it was hypothesised that haemodynamic graft performance could be quantified by the amount of disturbed flow in the venous segment $\tilde{u}_{\max}(t, \vec{x})$, the area exposed to non-physiological WSS metrics and by the pressure drop over the graft. While haemodynamics are believed to play an important role in graft performance, the exact haemodynamic trigger for NIH development is unknown.³ As such, the objective function used to quantify haemodynamic performance of each graft used equal weighting of each haemodynamic metric related to graft dysfunction. It is possible that an approach in which one or more of individual objective functions are prioritised over the others could result in different optimisation results. However, to establish such a prioritisation more insights into the exact relation between haemodynamics and graft dysfunction are required. Nonetheless, because the proposed objective function targets multiple haemodynamic metrics, it is likely that minimisation of the objective function can maintain an overall haemodynamic benefit even when future insights in the development of NIH would invalidate one of the hypotheses used in this study.

Using the meta-modelling approach, haemodynamic metrics for graft performance were generally well predicted. However, it was observed that the discrepancy between the CFD simulation and the meta-model-based predictions of % $WSS_{>7Pa}$ and $OSI_{>0.25}$ were outside the estimated meta-model uncertainty domains. A possible explanation for this discrepancy could be that the leave-one-out cross validation coefficients of both meta-models were relatively low (i.e., <0.9). This coefficient could potentially be increased by increasing the size of the meta-model training set, which would, in result, reduce the discrepancy between the meta-model prediction and the CFD simulation. However, even though a large discrepancy was found between the meta-model prediction and the CFD simulation result, haemodynamic performance of the optimised graft was better than that of the best performing graft in the meta-model training dataset, thereby demonstrating the general applicability of our optimisation approach.

In this study, a Newtonian blood model was used. As such, the shear thinning behaviour of blood, which can occur in regions of low shear-rates and high flow residence-times³² may be neglected. However, in the simulations performed in this study flow velocities are high throughout most of the computational domain, which, in general, will result in high shear-rates. Furthermore, it is expected that because of the high AVG flow rates, flow residence-times in regions of low shear-rates will be low. Consequently, it is hypothesised that in the context of the AVG simulations performed in this study, the use of a Newtonian blood model is warranted. Nonetheless, the impact of a non-Newtonian blood model on simulation results should be investigated in a future study.

4.2 | Conclusion

In this study an efficient meta-modelling technique was used to propose an optimised AVG design. It was demonstrated that the meta-modelling approach used in this study could be successfully applied to efficiently identify an optimised

AVG. Using CFD simulations, it was subsequently confirmed that the identified optimal graft design indeed showed a haemodynamic benefit over a standard straight graft. Future studies should evaluate the haemodynamic performance of the proposed graft design in a larger set of patient-specific CFD simulations.

ACKNOWLEDGEMENTS

This work was performed under the framework of Chemelot InSciTe (Grant number: BM1.01) This work was carried out on the Dutch national e-infrastructure with the support of SURF Cooperative (Grant number: muc16272).

CONFLICT OF INTEREST

No benefits in any form have been or will be received from a commercial party related directly or indirectly to the subject of this manuscript.

ORCID

Sjeng Quicken  <https://orcid.org/0000-0002-4496-3998>

Tammo Delhaas  <https://orcid.org/0000-0001-6897-9700>

Barend M. E. Mees  <https://orcid.org/0000-0001-6545-5813>

Wouter Huberts  <https://orcid.org/0000-0002-0779-4785>

REFERENCES

- Lee T, Haq NU. New developments in our understanding of Neointimal hyperplasia. *Adv Chronic Kidney Dis*. 2015;22(6):431-437. <https://doi.org/10.1053/j.ackd.2015.06.010>.
- Roy-Chaudhury P, Kelly BS, Miller MA, et al. Venous neointimal hyperplasia in polytetrafluoroethylene dialysis grafts. *Kidney Int*. 2001; 59(6):2325-2334. <https://doi.org/10.1046/j.1523-1755.2001.0590062325.x>.
- Cunnane CV, Cunnane EM, Walsh MT. A review of the hemodynamic factors believed to contribute to vascular access dysfunction. *Cardiovasc Eng Technol*. 2017;8(3):280-294. <https://doi.org/10.1007/s13239-017-0307-0>.
- Moufarrej A, Tordoir J, Mees B. Graft modification strategies to improve patency of prosthetic arteriovenous grafts for hemodialysis. *J Vasc Access*. 2016;17:S85-S90. <https://doi.org/10.5301/jva.5000526>.
- Stonebridge PA, Brophy CM. Spiral laminar flow in arteries? *Lancet*. 1991;338(8779):1360-1361. [https://doi.org/10.1016/0140-6736\(91\)92238-W](https://doi.org/10.1016/0140-6736(91)92238-W).
- Liu X, Pu F, Fan Y, Deng X, Li D, Li S. A numerical study on the flow of blood and the transport of LDL in the human aorta: the physiological significance of the helical flow in the aortic arch. *Am J Physiol Heart C Physiol*. 2009;297(1):H163-H170. <https://doi.org/10.1152/ajpheart.00266.2009>.
- Gallo D, Steinman DA, Bijari PB, Morbiducci U. Helical flow in carotid bifurcation as surrogate marker of exposure to disturbed shear. *J Biomech*. 2012;45(14):2398-2404. <https://doi.org/10.1016/j.jbiomech.2012.07.007>.
- Caro CG, Cheshire NJ, Watkins N. Preliminary comparative study of small amplitude helical and conventional ePTFE arteriovenous shunts in pigs. *J R Soc Interface*. 2005;2(3):261-266. <https://doi.org/10.1098/rsif.2005.0044>.
- Stonebridge PA, Vermassen F, Dick J, Belch JFF, Houston G. Spiral laminar flow prosthetic bypass graft: medium-term results from a first-in-man structured registry study. *Ann Vasc Surg*. 2012;26(8):1093-1099. <https://doi.org/10.1016/j.avsg.2012.02.001>.
- Huijbregts HJTAM, Blankestijn PJ, Caro CG, et al. A helical PTFE arteriovenous access graft to swirl flow across the distal anastomosis: results of a preliminary clinical study. *Eur J Vasc Endovasc Surg*. 2007;33(4):472-475. <https://doi.org/10.1016/j.ejvs.2006.10.028>.
- van Canneyt K, Morbiducci U, Eloit S, De Santis G, Segers P, Verdonck P. A computational exploration of helical arterio-venous graft designs. *J Biomech*. 2013;46(2):345-353. <https://doi.org/10.1016/j.jbiomech.2012.10.027>.
- Ruiz-Soler A, Kabinejadian F, Slevin MA, Bartolo PJ, Keshmiri A. Optimisation of a novel spiral-inducing bypass graft using computational fluid dynamics. *Sci Rep*. 2017;7(1):1-14. <https://doi.org/10.1038/s41598-017-01930-x>.
- Kabinejadian F, McElroy M, Ruiz-Soler A, et al. Numerical assessment of novel helical/spiral grafts with improved hemodynamics for distal graft anastomoses. *PLoS One*. 2016;11(11):e0165892. <https://doi.org/10.1371/journal.pone.0165892>.
- Fang K-T, Li R, Sudjianto A. *Design and Modeling for Computer Experiments*. New York, NY: Chapman and Hall/CRC; 2005.
- Blatman G, Sudret B. An adaptive algorithm to build up sparse polynomial chaos expansions for stochastic finite element analysis. *Probabilistic Eng Mech*. 2010;25(2):183-197.
- Quicken S, Donders WP, van Disseldorp EMJ, et al. Application of an adaptive polynomial chaos expansion on computationally expensive three-dimensional cardiovascular models for uncertainty quantification and sensitivity analysis. *J Biomech Eng*. 2016;138(12): 121010. <https://doi.org/10.1115/1.4034709>.
- Sudret B. Global sensitivity analysis using polynomial chaos expansions. *Reliab Eng Syst Saf*. 2008;93(7):964-979. <https://doi.org/10.1016/j.ress.2007.04.002>.
- Antiga L, Piccinelli M, Botti L, Ene-Iordache B, Remuzzi A, Steinman DA. An image-based modeling framework for patient-specific computational hemodynamics. *Med Biol Eng Comput*. 2008;46(11):1097-1112. <https://doi.org/10.1007/s11517-008-0420-1>.

19. Antiga L, Ene-Iordache B, Caverni L, Cornalba GP, Remuzzi A. Geometric reconstruction for computational mesh generation of arterial bifurcations from CT angiography. *Comput Med Imaging Graph*. 2002;26(4):227-235. [https://doi.org/10.1016/S0895-6111\(02\)00020-4](https://doi.org/10.1016/S0895-6111(02)00020-4).
20. Zheng T, Fan Y, Xiong Y, Jiang W, Deng X. Hemodynamic performance study on small diameter helical grafts. *ASAIO J*. 2009;55(3):192-199. <https://doi.org/10.1097/MAT.0b013e31819b34f2>.
21. Sobol IM. On the distribution of points in a cube and the approximate evaluation of integrals. *USSR Comput Math Math Phys*. 1967;7(7):86-112.
22. Mortensen M, Valen-Sendstad K. Oasis: a high-level/high-performance open source Navier-stokes solver. *Comput Phys Commun*. 2015;188:177-188. <https://doi.org/10.1016/j.cpc.2014.10.026>.
23. Logg A, Mardal K, Wells GN. In: Logg A, Mardal K-A, Wells G, eds. *Automated Solution of Differential Equations by the Finite Element Method*. Berlin Heidelberg, Germany: Springer Berlin Heidelberg; 2012.
24. Smith NP, Pullan AJ, Hunter PJ. An anatomically based model of transient coronary blood flow in the heart. *SIAM J Appl Math*. 2002;62(3):990-1018. <https://doi.org/10.1137/S0036139999355199>.
25. Malek AM, Alper SL, Izumo S. Hemodynamic shear stress and its role in atherosclerosis. *JAMA*. 1999;282(21):2035-2042. <https://doi.org/10.1001/jama.282.21.2035>.
26. Fry DL. Acute vascular endothelial changes associated with increased blood velocity gradients. *Circ Res*. 1968;22(2):165-197. <https://doi.org/10.1161/01.RES.22.2.165>.
27. He X, Ku DN. Pulsatile flow in the human left coronary artery bifurcation: average conditions. *J Biomech Eng*. 1996;118(1):74-82. <https://doi.org/10.1115/1.2795948>.
28. Crestaux T, le Maître O, Martinez J-M. Polynomial chaos expansion for sensitivity analysis. *Reliab Eng Syst Saf*. 2009;94(7):1161-1172.
29. Xiu D, Karniadakis GEM. The wiener-Askey polynomial chaos for stochastic differential equations. *SIAM J Sci Comput*. 2002;24(2):619-644.
30. Keshmiri A, Ruiz-Soler A, McElroy M, Kabinejadian F. Numerical investigation on the geometrical effects of novel graft designs for peripheral artery bypass surgery. *Procedia CIRP*. 2016;49:147-152. <https://doi.org/10.1016/j.procir.2015.11.005>.
31. Grechy L, Iori F, Corbett RW, et al. Suppressing unsteady flow in arterio-venous fistulae. *Phys Fluids*. 2017;29(10):101901. <https://doi.org/10.1063/1.5004190>.
32. Arzani A. Accounting for residence-time in blood rheology models: do we really need non-Newtonian blood flow modelling in large arteries? *J R Soc Interface*. 2018;15(146):20180486. <https://doi.org/10.1098/rsif.2018.0486>.

How to cite this article: Quicken S, Delhaas T, Mees BME, Huberts W. Haemodynamic optimisation of a dialysis graft design using a global optimisation approach. *Int J Numer Meth Biomed Engng*. 2021;37:e3423. <https://doi.org/10.1002/cnm.3423>